Applied and Environmental Microbiology, Feb. 2011, p. 1493–1500 Vol. 77, No. 4
0099-2240/11/$12.00 doi:10.1128/AEM.02233-10

Spatial Distribution of Bacterial Colonies in a Model Cheese▽

S. Jeanson,[1,2]* J. Chadœuf,[3] M. N. Madec,[1,2] S. Aly,[1,2] J. Floury,[1,2] T. F. Brocklehurst,[4] and S. Lortal[1,2]

INRA, UMR1253, F-35000 Rennes, France[1]; Agrocampus Ouest, UMR1253, F-35000 Rennes, France[2]; INRA, UR546 BioSP, F-84914 Avignon, France[3]; and Institute of Food Research, Norwich Research Park, Norwich NR4 7UA, United Kingdom[4]

Received 20 September 2010/Accepted 8 December 2010

In most ripened cheeses, bacteria are responsible for the ripening process. Immobilized in the cheese matrix, they grow as colonies. Therefore, their distribution as well as the distance between them are of major importance for ripening steps since metabolites diffuse within the cheese matrix. No data are available to date about the spatial distribution of bacterial colonies in cheese. This is the first study to model the distribution of bacterial colonies in a food-type matrix using nondestructive techniques. We compared (i) the mean theoretical three-dimensional (3D) distances between colonies calculated on the basis of inoculation levels and considering colony distribution to be random and (ii) experimental measurements using confocal microscopy photographs of fluorescent colonies of a *Lactococcus lactis* strain producing green fluorescent protein (GFP) inoculated, at different levels, into a model cheese made by ultrafiltration (UF). Enumerations showed that the final numbers of cells were identical whatever the inoculation level (10^4 to 10^7 CFU/g). Bacterial colonies were shown to be randomly distributed, fitting Poisson's model. The initial inoculation level strongly influenced the mean distances between colonies (from 25 μm to 250 μm) and also their mean diameters. The lower the inoculation level, the larger the colonies were and the further away from each other. Multiplying the inoculation level by 50 multiplied the interfacial area of exchange with the cheese matrix by 7 for the same cell biomass. We finally suggested that final cell numbers should be discussed together with inoculation levels to take into account the distribution and, consequently, the interfacial area of colonies, which can have a significant influence on the cheese-ripening process on a microscopic scale.

During cheese making, regardless of the cheese type, bacteria are immobilized in the curd during the coagulation step. It is generally accepted that 90% of the bacteria present in the milk are retained, trapped in the curd, while only 10% are lost in the whey during draining (16). In cheeses made by ultrafiltration (UF), the draining step is absent, and 100% of the cells are then retained in the curd. In any case, after immobilization by coagulation, each inoculated bacterial cell is assumed to grow, generating a colony inside the curd. Colonies are then spread within the cheese curd, and they interact with the cheese matrix during ripening. Consequently, the ripening process must take place on a microscopic scale around colonies. Only studies showing microscopic examinations of bacterial colonies in cheese either by electronic microscopy (24) or, more recently, by confocal laser scanning microscopy (7, 19) have been reported.

The ripening process (proteolysis, lipolysis, amino acid catabolism, and the production of organic acids, etc.) relies on the metabolic activities of bacterial colonies, leading to the formation of flavors and textures of cheese (11, 25). So far, ripening has always been described with average processes on the cheese scale with destructive techniques like grinding (5, 12, 23) or slicing (10), and microgradients of nutrients and metabolites are thus assumed to occur between colonies in the cheese matrix. Ripening process kinetics should then depend not only on the activities of colonies but also on the spatial organization of colonies inside the matrix. Currently, there are no quantitative data about the spatial distribution of bacterial colonies within a cheese matrix or any other food-like matrix. Our hypothesis is that the distance between colonies is a crucial parameter to understand cheese ripening. Our hypothesis is based on (i) that the distribution of colonies will change the distribution of bacterial enzymes in the cheese matrix and (ii) that interactions between colonies will be modulated by the distance between them, as metabolites must diffuse from one colony to its neighbor.

The distribution of immobilized bacteria in food has been described on a macroscopic scale both for minced meat, by grinding meat samples (27), and for Cheddar cheese blocks, by cutting cheese sections (29), using destructive techniques. Maps of the average cell numbers for each neighbor section were then drawn to describe the macroscopic distribution of bacteria in Cheddar cheese. In minced meat, theoretical Poisson and gamma Poisson distributions were fitted to experimental data in order to determine how many steps of grinding were necessary to obtain a random distribution of pathogens. It was finally not clear which one of these two models of distribution was the most accurate for this objective (35). In cheese, bacteria are immobilized after a long stirring step and the coagulation step. The spatial repartition of colonies should then depend on the distribution of bacterial cells at the end of the immobilization step, on the spatial distribution of nutrients, and on the interactions between colonies. If bacteria are not well mixed in milk before being immobilized or if the matrix is not homogeneous, so that some regions are favorable for bacterial growth (a high concentration of nutrients, for example) or so that bacteria cannot grow in one of the components of the matrix (the fat phase, for example), then an aggregative distribution, for example, a Neyman-Scott distribution (9),

* Corresponding author. Mailing address: INRA-UMR STLO, 65 Rue de Saint-Brieuc, 35042 Rennes Cedex, France. Phone: 33 (0) 223 485 337. Fax: 33 (0) 223 485 350. E-mail: sophie.jeanson@rennes.inra.fr.

▽ Published ahead of print on 17 December 2010.

would be expected. If colonies compete for nutrients very early, not all immobilized cells would have developed as a colony, and a regular repartition of colonies is then expected, such as a Gibbs model distribution (9). Finally, in a homogeneous matrix with an excess of nutrients (lactose and proteins, etc.), no interaction is suspected, at least at the beginning of development, and a complete random distribution is then expected, such as a Poisson distribution (9).

In 1995 (3, 40), the growth of bacterial colonies started to be described for model systems (gelatin or agar media) by measuring the colony surface in transparent medium. The immobilization of two species of pathogenic bacteria, growing as colonies in a solid-cheese-like medium, was shown to decrease the growth rates in comparison with those for liquid milk cultures (32). Therefore, the predictive models of growth in liquid are generally inaccurate for immobilized bacteria, as was shown previously for several bacterial species by Wilson et al. (39). Mean theoretical distances between colonies according to their inoculation level were calculated based on the hypothesis that they were randomly distributed (34). The surface of colonies grown in agar was positively correlated to the mean theoretical distance between colonies.

The present study is the first one to experimentally assess bacterial colony distribution/size in a solid-food matrix using a model system (gel cassette) and nondestructive techniques. The objective of the present work was to provide, for the first time, quantitative experimental data regarding the distribution of bacterial colonies in cheese, depending on the level of inoculation. An optical distortion was revealed by the experimental data with confocal microscopy and was taken into account in the mathematical treatment. Theoretical calculations were first performed and then experimentally validated by using stacked photographs taken with a confocal microscope and statistical image analysis. Because cheese matrices made by UF are homogeneous matrices, with high concentrations of lactose, we tested a random distribution of colonies.

MATERIALS AND METHODS

Strain and growth conditions. A *Lactococcus lactis* strain producing green fluorescent protein (GFP) was chosen to visualize lactococcal colony distribution in a cheese matrix. *L. lactis* subsp. *cremoris* MG1363 (38) carrying plasmid pJIM2246:*gfp* was provided by Marie-Pierre Chapot-Chartier (Micalis, INRA, Jouy-en-Josas, France). Briefly, it was obtained by transferring the transcriptional fusion of the *ldhL* promoter with *gfp* (described by Gory et al. [13]) in the pJIM2246 vector (28). This allows the constitutive expression of GFP under the transcriptional control of the *Lactobacillus sakei* promoter of the lactate dehydrogenase gene (*ldh*). The emission of GFP is then linked to the metabolically active state of the cells. *L. lactis* MG1363(pJIM2246:*gfp*) was stored at −80°C in 15% (vol/vol) glycerol and was first precultured twice in M17 (Difco, Becton Dickinson, Le Pont de Claix, France) supplemented with 0.5% glucose plus 10 μg/ml of chloramphenicol and incubated overnight at 30°C. Because the MG1363 strain has been cured of all its plasmids (38), this strain is a lactose-negative (lac^-) and proteinase-negative ($prtP^-$) strain.

The preculture grown overnight was used to inoculate the ultrafiltration (UF) retentate to targeted inoculation levels of 10^4 CFU/g, 10^5 CFU/g, 10^6 CFU/g, and 10^7 CFU/g. The initial inoculation levels in the gel cassettes were finally measured at 2.1×10^4 CFU/g, 2.0×10^5 CFU/g, 1.6×10^6 CFU/g, and 9.2×10^6 CFU/g by plating enumerations on M17 plates incubated for 48 h at 30°C.

Microfiltration and ultrafiltration of milk. The UF retentate was produced from microfiltrated milk to remove the indigenous microflora as described previously by Ulvé et al. (37), except that no NaCl and no cream were added, giving a nonsalty and nonfatty retentate. Briefly, microfiltration pilot equipment was used with skimmed milk heated at 50°C. It was equipped with 19 P1940 units (Pall-Exekia, Bazet, France) and 4.6 m^2 of Sterilox mineral membranes (0.8-μm pore size). The microfiltrate was then ultrafiltrated using pilot equipment (TIA, Bollene, France) equipped with 13.6 m^2 of mineral membranes with a molecular mass cutoff of 8 kDa (Tami, France).

The total proteins of milk were concentrated 4.2 times, and the retentate composition was as follows: 208.5 g/kg dry matter, 146.4 g/kg total nitrogen, 27.8 g/kg noncasein nitrogen, and 1.73 g/kg nonprotein nitrogen. The pH was 6.64 (±0.01). The UF retentate obtained was stored at −20°C in sterile plastic bottles.

Model cheese making. The UF retentate (35 ml per gel cassette) was thawed at 4°C overnight and then at 48°C 20 min before use.

The UF retentate was stirred, heated up to 93°C for 15 min, and immediately placed into melting ice for 3 min with manual stirring. The temperature dropped to 30°C.

The coagulant agent Maxiren 180 (DSM Food Specialties, France) was 1/10 diluted in sterile water and immediately added at a final concentration of 0.03% into the UF retentate. After inoculation of the strain, the mixture was manually and vigorously stirred for more than 2 min to reach the best possible homogenization.

Preparation of gel cassettes. The gel cassette system (2, 4) was used, as it allows nondestructive microscopic examinations. The cassette is constituted with an acetate frame 2 mm thick with an open window of 10 cm by 10 cm sealed within a sleeve of polyvinyl chloride (PVC) that is 15 μm thick and gas permeable. The whole system was autoclaved at 110°C for 15 min.

About 35 ml of the above-described mixture (retentate plus coagulant agent plus strain) was slowly poured into the gel cassette by the aid of a 50-ml syringe from the top of the frame inside the PVC sleeve. The gel cassette was then vertically incubated at 30°C for 1 h, clamped within a supporting frame that had a Perspex front to prevent the distortion of the cassette. This ensured that the thickness of the coagulated retentate within had a regular thickness of 2 mm. After 1 h, the clamps were removed, and the gel cassettes were incubated horizontally (with air access on both sides) at 19°C for 3 days to avoid syneresis. Before microscopic examination, the gel cassettes were stored at +4°C in order to increase oxygen dissolution in the retentate and improve the GFP fluorescence efficiency.

Confocal microscopy. The microstructural analysis was performed by using an Eclipse-TE2000-C1si inverted microscope (Nikon, Champigny-sur-Marne, France), allowing confocal laser scanning microscopy (CLSM). Confocal experiments were performed by using an argon laser operating at a 488-nm excitation wavelength (emission was detected between 500 and 530 nm). The gel cassettes were examined directly under the confocal microscope without any specific preparation. For all gel cassettes, a lens with a ×10 magnification was used without immersion. The optical field was 1,300 by 1,300 μm. For the gel cassettes inoculated at 1.6×10^6 and 9.2×10^6 CFU/g, a lens with a ×20 magnification was also used, with an optical field of 636 by 636 μm and oil immersion. With the ×10 magnification, small colonies could not be detected. GFP fluorescence was excited with a 488-nm laser fixed at 10% intensity. The detector rate at 515 nm ranged from 6.9 to 7.5 in order to optimize the detection of colonies among the autofluorescence of the UF retentate.

Stacks of photographs were taken under the microscope from the surface of the gel cassette through the PVC film into its depth (100 to 200 μm deep) by 2-μm steps (50 to 100 photographs per stack). At least 12 stacks were taken for each gel cassette by scanning the surface of the 10- by 10-cm gel cassette, leading to a total of about 7,000 photographs.

Calculations of mean theoretical distances. For calculations of mean theoretical distances, we did not use any experimental data.

Based on the assumption that the colonies were evenly distributed at a given density of colonies, i.e., the mean number of colonies per unit volume, mean three-dimensional (3D) distances (d_3) were calculated from center to center with the following equations:

$$d_3(\lambda) = \frac{1}{\sqrt[3]{\lambda}} d_3 \tag{1}$$

$$d_3 = 4\pi \int_{u>0} u^3 e^{-\frac{4}{3}\pi u^3} du \tag{2}$$

The first equation can be understood as a scale change: if the length unit is multiplied by a constant (a), then the distance between neighboring colonies is divided by a, while the number of colonies per unit volume is multiplied by a^3. The second equation comes from the fact that the probability of finding no particle inside the sphere of the radius (u) is as follows:

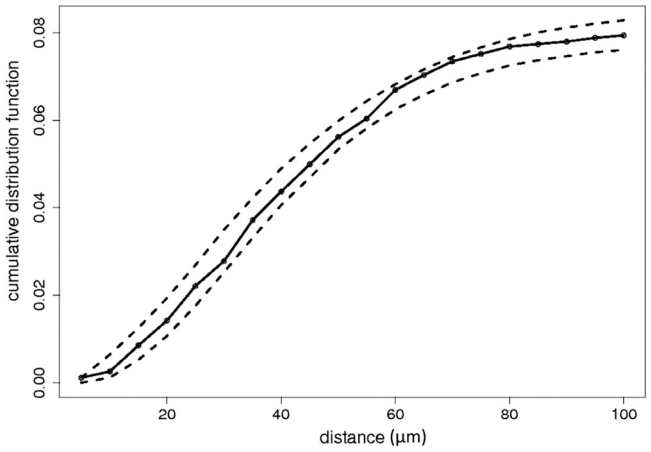

FIG. 1. Test of random repartition of colony sections. Black curve, cumulative distribution function of the distance between a colony and its nearest neighbor; dashed curves, individual confidence band at the 5% level.

$$e^{-(4/3)\pi u^3} \tag{3}$$

for a Poisson point process of intensity 1 (31).

Image analysis of experimental photographs. (i) Evaluation of the optical distortion to be introduced into the mathematical model. Fluorescent polystyrene beads (spheres) with a 15-μm diameter (FluoSpheres; Invitrogen, Cergy-Pontoise, France) were inoculated into the cheese and observed under the same conditions in order to clarify the distortion of colonies observed with the confocal microscope (see Results, and for further details, see the Appendix).

(ii) Selection of bacterial colonies among autofluorescent components. Colonies appeared on each photograph as fluorescent components, i.e., groups of connected pixels with a higher intensity than that of their surroundings (see the Appendix). However, cheese matrix autofluorescence generated random noise, with pixels of high intensity randomly spread in the image, so some fluorescent components of high intensity could also be due to autofluorescence. To optimize the detection of bacterial colonies, we chose photographs at a level maximizing the contrast between colonies and background.

(a) Step 1: selection of analyzed photographs from stacks. Two photographs per stack were thus chosen. The selected photographs were separated by 30 μm so that they could be considered an independent repetition, since colonies could not intercept both photographs. More than 120 photographs were all analyzed as ".tif" files with R software (26).

(b) Step 2: detection of fluorescent components. We applied an intensity threshold at an intensity level of 0.1 so that pixels under this threshold were considered background. This threshold was performed since choosing images with a high level of contrast was not sufficient to suppress random noise due to autofluorescence. The 0.1 threshold was chosen so that all components larger than 2 pixels were removed. We then selected fluorescent components of more than 3 pixels to potentially be colonies. Components with fewer than 3 pixels were considered to be autofluorescence. We estimated the intensity distribution, "*g*," of one pixel using all these fluorescent components with fewer than 3 pixels.

(c) Step 3: extraction of colonies among fluorescent components. Colony components differ from autofluorescent components by the fact that the intensity of each one of their constitutive pixels should be higher than that of the autofluorescent ones and more homogeneous between pixels (see Fig. A1 in the Appendix). We then tested if a component of "*j*" pixels was a colony by testing if its total intensity (defined as the sum of the intensities of its pixels) was greater than the expected value under the autofluorescence intensity distribution, "*g*," at the 1% level. This threshold was validated by visually and/or manually confirming several hundred detected components as being real colonies.

(iii) Test of complete random spatial distribution of colonies. As colonies were assumed to be independently uniformly and randomly spread in space, we tested the random spatial distribution, which is an essential prerequisite to estimate colony radius and colony density in cheese. The estimation is presented below in the next paragraph. The assumption of a random uniform distribution of colony centers is fulfilled as soon as bacteria are initially randomly spread in the cheese matrix by the stirring step before coagulation and because colonies are assumed to develop independently from each other. If this assumption is fulfilled, then the centers of colony sections are randomly uniformly spread in the section plane. This consists of testing (9) whether the cumulative distribution function of the distance between a colony section center and its nearest neighbor lies within its confidence band (Fig. 1). This confidence band was obtained by randomly redistributing the centers of the colony section within their sections (9).

(iv) Estimation of colony diameter probability density and colony density. Bacterial colonies in the cheese matrix are modeled as a Boolean model (22), supposing that (i) colony centers are Poisson distributed and (ii) colonies are spheres with a random independent radius, *r*. This model is characterized by the density of colonies (λ) and the probability density of the radius, $a(r)$. Fluorescent colonies observed in space under the confocal microscope appeared to be deformed. They followed a Boolean model with the same mean number of colony centers, but deformed colonies were modeled by ellipsoids of axis length ($2r$, $2r$, and $2kr$), where k is the anisotropy ratio (see Results) and $2r$ is the colony diameter (17).

The sections of colonies in confocal photographs were then modeled as the Boolean process of disks obtained by the intersection of this Boolean model of ellipsoids with a horizontal plane. Its mean number of disk centers per unit area and the probability density of the disk radius as functions of k, λ, and $a(r)$ are given in the Appendix.

Estimations of λ and $a(r)$ were performed by the method of maximum of likelihood (6), after modeling $a(r)$ as a step function, the definition of which is as follows:

$$a(r) = \sum_{i \geq 0} a_i 1_{[\delta i \leq r < \delta(i+1)]} \tag{4}$$

Confidence bands were obtained by block bootstrap (18).

RESULTS

Theoretical spatial distribution of colonies by mathematical calculation. In order to visualize how the theoretical distribution

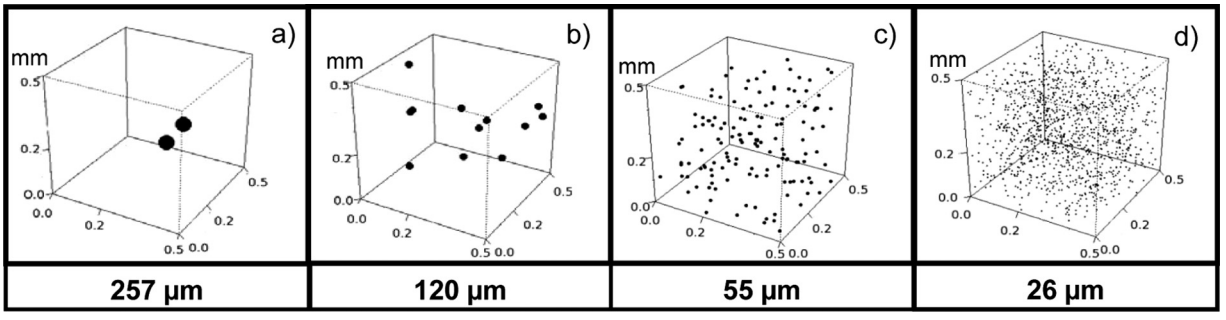

FIG. 2. Theoretical distribution of bacterial colonies in a volume (0.5 by 0.5 by 0.5 mm), such as a piece of cheese, assuming that they are evenly distributed at 10^4 CFU/cm^3 (a), 10^5 CFU/cm^3 (b), 10^6 CFU/cm^3 (c), and 10^7 CFU/cm^3 (d), and associated mean 3D theoretical distances to the nearest neighbor colony.

TABLE 1. Experimental data[a]

Inoculation level (CFU/g)	Observed values from image analysis[b]		Values calculated from observed values	
	Observed density[c] (λ) (colonies/cm^3)	Avg diam ($2r$) (μm) (±σ)	3D distance (d_3) (μm)	Interfacial area (S) (cm^2/cm^3)
2.1×10^4	NA	NA		
2.0×10^5	0.90×10^5	10.4 (2.6)	123	1.32
1.6×10^6	1.38×10^6	5.2 (1.6)	50	5.19
9.6×10^6	4.45×10^6	4.0 (0.5)	34	9.49

[a] Shown are enumerations, average densities of colonies per cm^3 (λ) and average diameters ($2r$) computed from the photographs using the mathematical model, average 3D distances (d_3) between the nearest neighbor colonies, and interfacial areas (S) of colonies calculated from λ and $2r$, respectively.
[b] NA, not analyzed because of too few colonies in each photograph.
[c] A value of 1 cm^3 can be considered 1 g in retentate cheese.

of colonies in a volume should be according to the inoculation level, we performed theoretical calculations and representations.

Figure 2 shows the theoretical distribution of colonies in a constant volume, a cube of cheese, for example, when cells are inoculated at 10^4 to 10^7 CFU/g. This 3D visualization brings to light the short distance between colonies when cells are inoculated at 10^7 CFU/g in comparison with an inoculation level of 10^4 CFU/g. The mean distance, $d_3(\lambda)$, from a colony center to the center of its nearest neighbor colony can be calculated (Fig. 2) based on the hypotheses that (i) all inoculated cells grow independently, each leading to a colony, and (ii) inoculated cells are randomly spread, fitting a Poisson distribution.

In a constant volume, depending on the level of inoculation, two colonies or hundreds of colonies can occur, giving a completely different environment in the food matrix. When the inoculation level was increased 1,000 times (from 10^4 to 10^7 CFU/g) the mean theoretical 3D distance decreased 10 times (Fig. 2) down to 26 μm, which is a very short distance between colonies. Space without bacterial activity was widely available when only two colonies occurred, while the space was completely covered by bacterial activity when hundreds of colonies occurred.

Distribution and size of lactococcal colonies in a model cheese depend on the level of inoculation determined by confocal microscopy examinations. We then wanted to check if colonies were truly randomly spread in the model cheese and if mean experimental distances between colonies fitted the mean theoretical ones.

Both the initial inoculation levels and the final numbers of cells after a 3-day incubation period at 19°C were measured by plating enumerations (Table 1). All the gel cassettes reached the same final number of cells, which was $(5.0 \pm 1.6) \times 10^8$ CFU/g, as well as the same final pH (pH 6.39 ± 0.01) whatever the initial inoculation level. These results have been confirmed by several preliminary experiments (data not shown).

Figure 3 shows the fluorescence emission produced by a strain producing GFP grown as colonies throughout a non-

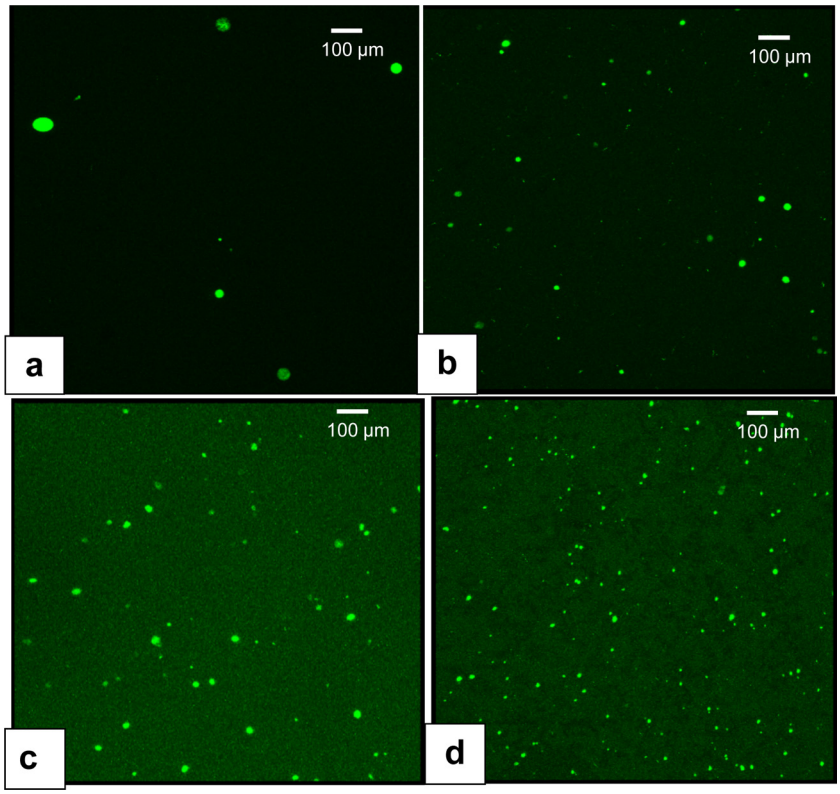

FIG. 3. Compilations in depth of stacked photographs (examples from 60 stacks) taken by confocal microscopy of gel cassettes filled with coagulated UF milk retentate and inoculated with a *Lactococcus* strain producing GFP at 2.1×10^4 (a), 2×10^5 (b), 1.6×10^6 (c), and 9.6×10^6 CFU/g (d), representing bacterial colonies grown in a 3D volume of a 120- to 150-μm depth by 1.3 by 1.3 mm.

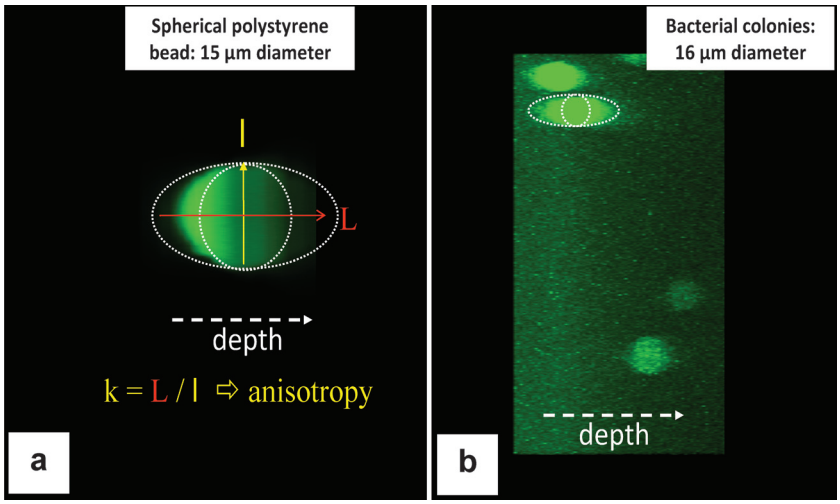

FIG. 4. Microscopic examination in the depth of the UF retentate (*z* compilation of tiled photographs) of a 15-µm fluorescent polystyrene bead (a) and bacterial colonies (b).

transparent matrix, such as milk UF retentate coagulated in gel cassettes. The inoculation level was a major influence on both the distribution of colonies and the mean diameter of colonies in the model cheese (Fig. 3). The observation of fluorescent colonies in the 7,000 photographs of the model cheese brought to light the correlation between the increasing number of colonies in a constant volume and the increasing inoculation level. It is also obvious that the mean size of colonies inside the model cheese increased when the number of colonies decreased and, at the same time, when the distance between colonies increased.

Spatial distribution of colonies in model cheese according to the inoculation level by statistical image analysis. The three highest levels of inoculation (2×10^5, 1.6×10^6, and 9.2×10^6 CFU/g) were statistically analyzed for one or two magnifications (120 photographs analyzed), while the inoculation level of 2.1×10^4 CFU/g had too few colonies in each photograph for statistics to be performed on them (Fig. 3).

Colonies were assumed to be independently spread out because inoculated cells were mixed as homogeneously as possible in the UF retentate. After selecting the fluorescent colonies among the background of the natural fluorescence of the retentate (see Materials and Methods), the hypothesis that colony centers followed a Poisson point process was not rejected at the 5% level for the three analyzed inoculation levels. We then concluded that colonies are randomly distributed in this nonfat model cheese.

On the basis of this hypothesis, both the density of colonies, λ, and the mean nearest 3D distances, d_3 (λ), between the neighbor colonies were computed (Table 1), taking into account the ellipsoid shape of colonies under the microscope by integrating the anisotropy ratio, *k*, into the calculation of the number of colonies per area (colonies in each photography). The initial inoculation levels measured by plating were always higher than the computed colony densities for the same inoculated cheese matrices (Table 1). This could be due to the low sensitivity of the enumeration technique (1). The computed colony densities may also have been underestimated because of the threshold values fixed for the intensity and size of the colonies. Hence, some small colonies may have been eliminated as background even if we visually and/or manually checked that the selection of colonies by the image analysis was accurate. However, even if the initial inoculation levels measured by plating were higher than the computed colony densities, both values were similar (maximum factor of 2). We can then conclude that all the inoculated cells gave rise to a colony in the cheese made by UF.

When the inoculation level was increased 50 times (inoculation level from 2.0×10^5 to 9.6×10^6 CFU/g), the mean diameters decreased 2.6 times. Table 1 confirms that colonies inoculated at a level between 10^6 and 5×10^6 CFU/g, which is the usual inoculation level in cheese making, are very close to each other (30 to 50 µm), confirming theoretical calculations. If the interfacial area (*S*) is the total surface (cm^2) of all the colonies per unit volume (cm^3), it corresponds to the total exchange surface between the bacterial colonies and the cheese matrix. The interfacial area was then multiplied by 7.2-fold (in cm^2/cm^3), with a 50-fold increase of the inoculation level. For the same increase in the inoculation level, the interfacial area, *S*, was multiplied with a much higher coefficient than the mean colony diameters, which means that the level of inoculation had a dramatic influence on the surface area of colonies in contact with the cheese matrix.

These statistical analyses could be performed only because we took into account in the mathematical model the optical distortion that we experienced by observing colonies under a confocal microscope.

Measurements of optical distortion. The assumption that colony sections can be represented by disks was tested by regressing the square root of the colony section areas on the colony section perimeters and testing that they are proportional with the parameter $1/2\sqrt{\pi}$. We accepted this assumption at the level of 5% in the *x* and *y* planes and rejected this assumption in the *x* and *z*, or *y* and *z*, planes (Fig. 4). If colonies are most likely spherical in 3D renderings, they are observed as ellipsoids on the *z* axis. This raises the question of the quantification of colony volume and distribution using measurements with image analyses by confocal microscopy. As the polysty-

rene beads also appeared as ellipsoids in the *z* axis, we confirmed that the ellipsoid image was an optical distortion (Fig. 4). Consequently, sections of colonies could be detected on photographs at depths where they were not actually present, which could lead to an overestimation of the number of colony sections in each photograph and then to an overestimation of the density of colonies, if not taken into account.

We then described the confocal observation of colonies as ellipsoids of axis length ($2r$, $2r$, and $2kr$), where k is the anisotropy ratio. The ratio k was calculated by the mean ratio of 30 random colonies at each inoculation level. The ratio k was constant (4.11 ± 0.3) whatever the size, the volume, and the density of colonies, confirming that the optical effect was probably due to the field depth of the lens independent of the observed object.

DISCUSSION

Bacteria immobilized in cheese grow as colonies, and they are mostly responsible for the ripening process. Ripening must then take place on a microscopic scale, between colonies, depending on the distance between colonies.

In this work, the spatial distribution of bacteria in cheese was described for the first time, using a real food matrix, in the form of a model cheese made by UF and a *Lactococcus* strain producing GFP. Bacterial colonies were shown to be randomly distributed. Quantitative data were provided regarding distances between colonies and sizes of colonies, depending on the level of inoculation, which had a crucial impact on spatial colony distribution. Mean distances calculated from the image analysis of experimental data fitted perfectly the theoretical calculations. At high levels of inoculation, colonies were extremely close to each other in the third dimension, since mean distances of 25 to 30 μm (Fig. 2 and Table 1) were obtained. Furthermore, the parameter that increased the most when the level of inoculation increased was the interfacial area, *S*.

In terms of methodology, we developed a nondestructive and *in situ* approach to investigate the spatial distribution of bacterial colonies in cheese on a microscopic scale. The gel cassette is a perfect tool to study immobilized bacterial colonies (20, 30, 33). In the present paper, for the first time, these gel cassettes were successfully adapted to a model food matrix instead of gelatin or agar medium. In the developed methodology, we also showed that the fluorescence emission from a strain producing GFP is sufficient enough to avoid any additional staining before confocal observations are made. This is the first time that a strain of *Lactococcus* expressing GFP has been observed under the microscope in a nontransparent food matrix, such as this model UF cheese matrix. We proved that it was possible to quantify fluorescence. This work demonstrates an optical effect on the *z* axis when bacterial colonies are observed, likely due to the confocal lens giving them an ellipsoid appearance. Such an effect should be taken into consideration if colony density has to be estimated from stacks and image analysis. The *Lactococcus* strain was a lactose-negative and proteinase-negative mutant, which most likely explains why the final cell number was limited to 10^8 CFU/g and did not reach the usual maximum level, which is around 10^9 CFU/g for a lactose-positive and proteinase-positive ($lac^+/prtP^+$) strain (15, 37), with no loss of viability before 7 days. Further assays using that strain should first reintroduce the lac/prtP plasmid. Nevertheless, we are convinced that the lower maximum population of this strain did not affect the main conclusions of the present study.

The inoculation level influenced the mean size of the colonies. As the same final number of cells was reached (10^8 to 10^9 CFU/g) regardless of the inoculation level, if the level of inoculation was 10^4 CFU/g, colonies should grow to 10^4 to 10^5 cells each, while if the inoculation level was 10^7 CFU/g, colonies should grow to only 10 to 100 cells each. Of course, these final numbers of cells per colony do not lead to the same size and/or surface of the colony. Recently, the measured surface of bacterial colonies was shown to be linearly correlated to the number of CFU/ml (14, 30). Therefore, the final number of cells indicates neither the number/distribution of active colonies in the matrix nor the interfacial area between colonies and the surface. A growing colony may be constituted of cells in different physiological states. Cells in the exponential growth phase were shown previously to grow at the outer layer of the colony (21), in contact with the matrix. This outer layer is thus most likely highly metabolically active. We can therefore assume that the larger the interfacial area, *S*, the higher the bacterial activity on the food matrix (ripening processes). From this point of view, increasing the interfacial area, *S*, by more than 7 times when cells are inoculated at 9.6×10^6 CFU/g instead of 2×10^5 CFU/g should accelerate ripening process kinetics. If the interfacial area, *S*, is wide at high inoculation levels, the mean distance between colonies is short, and bacterial activity is widespread in the cheese matrix. This is the first study to introduce this concept in food microbiology, although it is widely used in physicochemistry and medicine. We now think that the final number of cells in the cheese must be discussed together with the inoculation level, as the latter is more indicative of the distribution and the mean size of the colonies than is the final number of cells.

Metabolites from the ripening processes, such as nutrients and aroma precursors, must be diffusing into the matrix between bacterial colonies. Some metabolites were shown previously to be responsible for synergism and antagonism in immobilized bacterial cocultures (36). It is therefore very important to quantify these distances, as they also influence the interaction between bacterial colonies of the same species or of different species, such as lactic acid bacteria and pathogens (34) or ripening species in cheese. Very little data are available regarding the diffusion of small solutes in cheeses (10). Whatever the diffusion rate, the closer the colonies are, the less the matrix microstructure influences the diffusion between colonies.

Further work should investigate the microenvironment around colonies depending on their size and the composition of the cheese matrix. The spatial distribution of colonies should now be assessed in real cheeses as a factor influencing cheese-ripening kinetics. The addition of fat will create a heterogeneous matrix with two phases. Colonies may not be evenly distributed, as it was previously shown that bacterial colonies were located at the fat-protein interface (8, 19), and these were not spherical. The interfacial area would also be increased because of their shape. The Boolean process will then not be homogeneous. Modeling must take into account

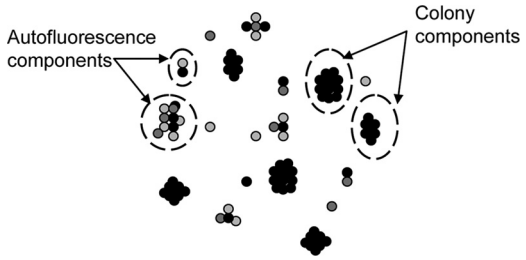

FIG. A1. Schematic representation of a confocal photograph with fluorescent components (groups of connected pixels) from bacterial colonies and from autofluorescence of the cheese matrix (background).

this nonhomogeneity by using, for example, inhomogeneous Boolean models directed by the phase structure.

The microenvironment of colonies can now be investigated *in situ* on a microscopic scale, monitoring different cheese-making and ripening processes or bacterial interactions within cheese matrices.

APPENDIX

To estimate the density of bacterial colonies on a photograph, we first differentiated the colony sections from the background and then estimated the density of colonies using a geometrical model of colonies.

Detecting colony sections. Colonies were detected by fluorescence and were characterized by groups of high-intensity pixels. However, the UF retentate within the gel cassettes was autofluorescent. This autofluorescence constituted the background. Therefore, we first thresholded it at intensity level of 0.1 so that pixels under this threshold were considered background. We then extracted the connected components composed of the remaining segments. These connected components were either colonies or groups of background fluorescent pixels.

The area distribution of these components was then expected to be a mixture of a sharply decreasing distribution and a unimodal distribution, whereas the distribution of the mean component intensity of small components was expected to be very variable due to the high variability of background pixels.

First, assuming that background pixels were spread at random on the photograph with independent fluorescence intensities, the area distribution of background-connected components was expected to be continuously decreasing, with a large variance of the mean fluorescence values for small components and a small variance for large components, even if the expected value of these mean values should be constant.

Second, supposing that bacterial colonies grew independently in a homogeneous medium, their section distribution was expected to be of a unimodal volume. The expectation of their mean fluorescence value was expected to be independent of the area of the section and larger than the expected area of the background components (Fig. A1).

Bacterial colonies were then estimated as components larger than an area threshold estimated as the value under which the sharp decrease of the area component distribution could no longer be detected and for which the P value of the mean fluorescence was lower than 0.01 under the assumption that it was a group of independent background pixels. This P value for each component was computed by using the fluorescence of components of one pixel as background pixels.

Estimating colony density and radius distribution. (i) Modeling of the colonies observed by confocal microscopy. We confirmed that the colonies were observed with the confocal microscope as ellipsoids, where the larger axis was in the z axis of the depth, the two other axes (x and y) were equal, and the ratio between axes (anisotropy) was constant. We tested whether colonies are spherical on the x and y axes. Being detected by their fluorescence, colonies that did not physically intercept a photograph at a given depth, but were near enough, could be optically detected on this photograph because of the ellipsoid shape in the z axis. We denote k the anisotropy ratio of the larger axis, z, and another axis (x or y) so that a colony of radius r is seen as an ellipsoid of axis lengths $2kR$, $2R$, and $2R$.

The following formulas are direct extensions of formulas obtained previously by Kok (17) for spheres and oblate ellipsoids.

(ii) Estimating the probability density of the colony radius. We assumed that if the colony distribution is random in the two-dimensional (2D) plane (on each photograph), it is also random in the 3D volume.

Therefore, the radius distribution of colonies has to be calculated on a 2D examination plane (i.e., one photograph of a stack). The observed section of a colony detected in the photograph and of radius R is a disk whose radius r on the photograph is random, and its probability density is as follows:

$$p(r) = \frac{r}{R^2} \frac{1}{\sqrt{1 - \frac{r^2}{R^2}}} \tag{A1}$$

If colony radii are random and $a(R)$ is the probability density of their radius, the radius r of a colony section on the photograph is random, and its probability density equates to the following:

$$p(r) = \frac{r}{\int_0^\infty Ra(R)dR} \int_r^\infty \frac{a(R)}{\sqrt{1 - \frac{r^2}{R^2}}} \frac{dR}{R} \tag{A2}$$

The probability density of the colony radii is then estimated by the maximum of likelihood (6), maximizing the probability, $\prod_{i=1}^{n} p(r_i)$, to observe the radii, $r_1, \ldots r_n$, observed for the colony sections.

(iii) Estimating the mean number of colonies per unit volume. The colonies growing from single bacteria uniformly and independently spread out in the model cheese matrix. The colony centers are modeled as a Poisson point process. Let λ be the mean number of colony centers per unit volume. The colony sections on an examined photograph follow a Poisson process with the mean number per unit area, μ, equating to the following:

$$\mu = 2k\lambda \int_0^\infty Ra(R)dR \tag{A3}$$

The mean number of colony sections per unit volume was then estimated by replacing the probability density of the colony radius by its estimation, replacing k by the mean of the measured values estimated directly for 30 independent colonies of various volumes and by replacing μ by an estimate equal to the number of observed disks divided by the total area of the sections.

Confidence intervals were obtained by block bootstrapping (18) of the observed sections, with a block being a quarter of a section.

(iv) Computing the distribution of the mean nearest distance between colony centers. With colony centers being Poisson distributed, the probability density of the distance (z) from one center to the center of its nearest neighbor depends only on the density of colonies per unit volume, with a probability density as follows:

$$p(z) = 4\pi \lambda z^2 \exp\left(-\frac{4}{3}\pi\lambda z^3 \right) \tag{A4}$$

Similarly, the probability density of the distance from the center of one colony section to the center of its nearest neighbor on the plane is equal to the following:

$$p(z) = 2\pi \mu z \exp(-4\pi\mu z^2) \tag{A5}$$

This depends only on μ, so it is a function of both λ and the colony radius distribution.

(v) Computing the interfacial area, S, per unit volume. With the mean number of colonies per unit volume being λ and the radius probability density of the colonies being $a(R)$, the mean interfacial area of the colonies per unit volume is as follows:

$$S = 4\pi\lambda \int_0^{\infty} R^2 a(R) dR \qquad \text{(A6)}$$

ACKNOWLEDGMENTS

We are very grateful to the team from our Pilot Plant for Research in Dairy Technology for producing and analyzing the UF-milk retentate. We are also extremely thankful to Marie-Pierre Chapot-Chartier (Micalis, INRA, Jouy-en-Josas, France) for kindly providing the *Lactococcus* strain producing GFP. We thank Anne Thierry and Valérie Gagnaire for reading our manuscript and providing helpful comments.

REFERENCES

1. **Augustin, J. C., and V. Carlier.** 2006. Lessons from the organization of a proficiency testing program in food microbiology by interlaboratory comparison: analytical methods in use, impact of methods on bacterial counts and measurement uncertainty of bacterial counts. Food Microbiol. **23:**1–38.
2. **Brocklehurst, T. F., A. R. Mackie, D. C. Steer, and P. D. R. Wilson.** April 1998. Detection of microbial growth. U.S. patent 5739003.
3. **Brocklehurst, T. F., G. A. Mitchell, Y. P. Ridge, R. Seale, and A. C. Smith.** 1995. The effect of transient temperatures on the growth of *Salmonella typhimurium* LT2 in gelatin gel. Int. J. Food Microbiol. **27:**45–60.
4. **Brocklehurst, T. F., R. B. Piggott, A. C. Smith, and D. C. Steer.** 1996. An apparatus for studying the effect of transient temperature on growth of bacteria in a gel matrix. Food Microbiol. **13:**109–114.
5. **Charlet, M., G. Duboz, F. Faurie, J.-L. Le Quéré, and F. Berthier.** 2009. Multiple interactions between *Streptococcus thermophilus*, *Lactobacillus helveticus* and *Lactobacillus delbrueckii* strongly affect their growth kinetics during the making of hard cooked cheeses. Int. J. Food Microbiol. **131:**10–19.
6. **Cox, D. R., and D. V. Hinkley.** 1974. Theoretical statistics. Chapman and Hall, London, United Kingdom.
7. **De Freitas, I., et al.** 2005. Microstructure, physicochemistry, microbial populations and aroma compounds of ripened Cantal cheeses. Lait **85:**453–468.
8. **De Freitas, I., et al.** 2007. In depth dynamic characterisation of French PDO Cantal cheese made from raw milk. Lait **87:**97–117.
9. **Diggle, P. J.** 2003. Statistical analysis of spatial point patterns. A. Hodder Arnold, London, United Kingdom.
10. **Floury, J., S. Jeanson, S. Aly, and S. Lortal.** 2010. Determination of the diffusion coefficients of small solutes in cheese: a review. Dairy Sci. Technol. **90:**477–508.
11. **Fox, P. F., T. K. Singh, and P. L. H. McSweeney.** 1995. Biogenesis of flavour compounds in cheese, p. 59–98. *In* E. L. Malin and M. H. Tunick (ed.), Chemistry of structure-function relationships in cheese. Plenum Press, New York, NY.
12. **Frazier, W. C., L. A. Burkey, A. J. Boyer, and G. P. Sanders.** 1935. The bacteriology of Swiss-type cheese. III. The relation of acidity of starters and of pH of the interior of Swiss cheeses to quality of cheeses. J. Dairy Sci. **18:**503–510.
13. **Gory, L., M.-C. Montel, and M. Zagorec.** 2001. Use of green fluorescent protein to monitor *Lactobacillus sakei* in fermented meat product. FEMS Microbiol. Lett. **194:**127–133.
14. **Guillier, L., P. Pardon, and J. C. Augustin.** 2006. Automated image analysis of bacterial colony growth as a tool to study individual lag time distributions of immobilized cells. J. Microbiol. Methods **65:**324–334.
15. **Hannon, J. A., et al.** 2006. Lysis of starters in UF cheeses: behaviour of mesophilic lactococci and thermophilic lactobacilli. Int. Dairy J. **16:**324–334.
16. **Jeanson, S.** 2000. Ph.D. thesis. Université de Bourgogne, Dijon, France.
17. **Kok, L. P.** 1990. 100 problems of my wife and their solution in theoretical stereology. Leyden, Netherlands.
18. **Lahiri, S. N.** 1999. Theoretical comparisons of block bootstrap methods. Ann. Stat. **27:**386–404.
19. **Lopez, C., M. B. Maillard, V. Briard-Bion, B. Camier, and J. A. Hannon.** 2006. Lipolysis during ripening of Emmental cheese considering organization of fat and preferential localization of bacteria. J. Agric. Food Chem. **54:**5855–5867.
20. **Malakar, P. K., et al.** 2000. Microgradients in bacterial colonies: use of fluorescence ratio imaging, a non-invasive technique. Int. J. Food Microbiol. **56:**71–80.
21. **McKay, A. L., A. C. Peters, and J. W. T. Wimpenny.** 1997. Determining specific growth rates in different regions of *Salmonella typhimurium* colonies. Lett. Appl. Microbiol. **24:**74–76.
22. **Molchanov, I.** 1997. Statistics of the Boolean model for practitioners and mathematicians. John Wiley & Sons, Chichester, United Kingdom.
23. **Pappa, E. C., I. G. Kandarakis, G. K. Zerfiridis, E. M. Anifantakis, and K. Sotirakoglou.** 2006. Influence of starter cultures on the proteolysis of Teleme cheese made from different types of milk. Lait **86:**273–290.
24. **Parker, M. L., P. A. Gunning, A. C. Macedo, F. X. Malcata, and T. F. Brocklehurst.** 1998. The microstructure and distribution of micro-organisms within mature Serra cheese. J. Appl. Microbiol. **84:**523–530.
25. **Rank, T. C., R. Grappin, and N. F. Olson.** 1985. Secondary proteolysis of cheese during ripening: a review. J. Dairy Sci. **68:**801–805.
26. **R Development Core Team.** 2008. R: a language and environment for statistical computing. R Foundation for Statistical Computing, Vienna, Austria.
27. **Reinders, R. D., R. De Jonge, and E. Evers.** 2003. A statistical method to determine whether micro-organisms are randomly distributed in a food matrix, applied to coliforms and *Escherichia coli* O157 in minced beef. Food Microbiol. **20:**297–303.
28. **Renault, P., G. Corthier, N. Goupil, C. Delorme, and S. D. Ehrlich.** 1996. Plasmid vectors for Gram-positive bacteria switching from high to low copy number. Gene **183:**175–182.
29. **Sheehan, A., G. O'Cuinn, R. J. Fitzgerald, and M. G. Wilkinson.** 2009. Distribution of microflora, intracellular enzymes and compositional indices throughout a 12 kg Cheddar cheese block during ripening. Int. Dairy J. **19:**321–329.
30. **Skandamis, P., T. Brocklehurst, E. Panagou, and G. Nychas.** 2007. Image analysis as a mean to model growth of *Escherichia coli* O157:H7 in gel cassettes. J. Appl. Microbiol. **103:**937–947.
31. **Stoyan, D., W. S. Kendall, and J. Mecke.** 2010. Stochastic geometry and its applications. Wiley, Chichester, United Kingdom.
32. **Theys, T., A. Geeraerd, and J. Van Impe.** 2009. Evaluation of a mathematical model structure describing the effect of (gel) structure on the growth of *Listeria innocua*, *Lactococcus lactis* and *Salmonella typhimurium*. J. Appl. Microbiol. **107:**775–784.
33. **Theys, T. E., A. H. Geeraerd, F. Devliehere, and J. F. Van Impe.** 2009. Extracting information on the evolution of the living- and dead-cell fractions of *Salmonella typhimurium* colonies in gelatin based on microscopic images and plate-count data. Lett. Appl. Microbiol. **49:**39–45.
34. **Thomas, L. V., J. W. T. Wimpenny, and G. C. Barker.** 1997. Spatial interactions between subsurface bacterial colonies in a model system: a territory model describing the inhibition of *Listeria monocytogenes* by a nisin-producing lactic acid bacterium. Microbiology **143:**2575–2582.
35. **Toft, N., G. T. Innocent, D. J. Mellor, and S. W. J. Reid.** 2006. The gamma-Poisson model as a statistical method to determine if micro-organisms are randomly distributed in a food matrix. Food Microbiol. **23:**90–94.
36. **Tsigarida, E., I. Boziaris, and G. Nychas.** 2003. Bacterial synergism or antagonism in a gel cassette system. Appl. Environ. Microbiol. **69:**7204–7209.
37. **Ulvé, V. M., et al.** 2008. RNA extraction from cheese for analysis of in situ gene expression of *Lactococcus lactis*. J. Appl. Microbiol. **105:**1327–1333.
38. **Wegmann, U., et al.** 2007. Complete genome sequence of the prototype lactic acid bacterium *Lactococcus lactis* subsp. *cremoris* MG1363. J. Bacteriol. **189:**3256–3270.
39. **Wilson, P. D. G., et al.** 2002. Modelling microbial growth in structured foods: towards a unified approach. Int. J. Food Microbiol. **73:**275–289.
40. **Wimpenny, J. W. T., et al.** 1995. Submerged bacterial colonies within food and model systems: their growth, distribution and interactions. Int. J. Food Microbiol. **28:**299–315.